Desalination and Water Treatment
www.deswater.com

doi: 10.1080/19443994.2013.781965

52 (2014) 102–110
January

Taylor & Francis
Taylor & Francis Group

Coagulation-dynamic membrane filtration process at constant flow rate for treating polluted river water

Chunhua Xu[a,*], Xiaohong Wang[a], Xiaoyun Dou[b], Baoyu Gao[a]

[a]*Shandong Key Laboratory of Water Pollution Control and Resource Reuse, School of Environmental Science and Engineering, Shandong University, No. 27 Shanda South Road, Jinan 250100, China*
Tel. +86 531 88362170; Fax: +86 531 88364513; email: xuchunhua@sdu.edu.cn
[b]*Environmental Protection School of Shandong Province, No. 12956 Jingshi Road, 250014 Jinan, China*

Received 19 December 2012; Accepted 26 February 2013

ABSTRACT

Dynamic membrane has attractive features, compared to the traditional membrane technology. This work investigated the performance and filtration process of a dynamic membrane (DM) at a constant flow rate, which was formed by flocs, produced by river water pollutants reacting with poly aluminum chloride with a non-woven fabric filter as the support media. Effluent turbidity was studied as the marker of a dynamic membrane formation, and chemical oxygen demand (COD) and total phosphorus (TP) were surveyed to evaluate the process performance. The results showed that the combined coagulation–dynamic membrane process is effective in treating polluted river water. The COD and TP removal efficiencies were obtained in the DM forming process and after formation. The relationship of the running pressure versus the operation time was used to evaluate the filtration process, according to the combined models of the membrane fouling. The standard model plays the dominant role in the first stage of the DM reactor running process, and after it, the intermediate model plays the leading role.

Keywords: Coagulation; Dynamic membrane; Filtration process; Constant flow rate; Non-woven fabric filter

1. Introduction

Dynamic membrane filtration has been increasingly used in the wastewater treatment process in recent years. Usually, the dynamic membrane is formed by exposing a mounted porous body to a solution, containing fine particles by a simple filtration process [1–3]. Compared with traditional membranes, inexpensive materials, high filtration flux, better filtration performance, and easy formation from various substances are very attractive features of dynamic membrane [4,5]. Therefore, it is considered as a substitute for the conventional membrane reactor [6,7].

Coagulation is an effective pretreatment, because it helps to remove the smallest particles. Thus, a combination of coagulation and dynamic membrane has been proposed. Small particles are destabilized and combined into larger aggregates, during the coagulation process. And it is removed from water, through the dynamic membrane. The combined process

*Corresponding author.

successfully integrates the advantages of both coagulation and membrane filtration.

The formation and filtration of particles of the dynamic membrane are similar to membrane fouling, resulting from the deposition of particles inside or on top of the membrane [8]. So, the four classical membrane fouling mechanisms are thus expected to be able to account for the formation and filtration processes of the dynamic membrane at constant flowrate [8–11]. The four models are: complete blocking model, intermediate blocking model, cake filtration model, and standard blocking model. The details of the four models are as follows: (i) complete blocking model, assuming that all particles seal off pore entrances, (ii) intermediate blocking model, assuming that a portion of particles seals off pores and the rest accumulate on top of other deposited particles, (iii) cake filtration model, assuming that particles accumulate on the surface of a membrane, in a permeable cake of increasing thickness that adds resistance to flow, and (iv) standard blocking model, assuming that particles accumulate on the walls of straight cylindrical pores inside membranes. But in actual process, Bolton [8] and Liu [11] think, only one model is not so ideal in simulating the real data and the theoretical model. So, the combined model was proposed as listed in Table 1.

Some efforts have been made to understand the formation and filtration mechanisms of the dynamic membrane, by means of fouling model analysis. Fan et al. [12] reported actual municipal wastewater with a self-forming dynamic membrane, formed on a coarse mesh, and the performance was satisfactory. The effluent suspended solid concentrations were undetectable in most cases, and chemical oxygen demand (COD) and the NH_3-N removal efficiencies averaged 84.2 and 98.03%, respectively. Sharp and Escobar [13] focused on testing different coagulation pretreatment techniques to improve membrane filtration in water separations. They believed that a coagulant-based dynamic membrane has the potential to be an effective method, to improve UF efficiency in water separation applications as well as to decrease pretreatment costs associated with the operation. Al-Malack et al. [14] investigated the effectiveness of a dynamic membrane made of woven fabric, in treating domestic wastewater, and the results showed that the membrane improved the overall performance of the crossflow microfiltration process. Y. Kiso created a dynamic membrane, in what they named a mesh filtration bio-reactor (MFBR) and used it to treat synthetic wastewater. The study revealed that the MFBR can be used as an alternative advanced wastewater treatment process [6]. A non-woven fabric filter was also evaluated as an alternative membrane for solid–liquid separation, in an activated sludge reactor, and showed good performance, sufficient for domestic wastewater treatment [5]. Zhang et al. [15] used the self-forming dynamic membrane bioreactor, to remove the contaminants in bleaching the effluent discharged from the straw pulping process, and the results showed the dynamic membrane formed normally in 60 min, the COD decreased obviously from 1,344 mg/L in the influent to 260 mg/L in the effluent, and lignin from 390 to 192 mg/L.

Above researches indicate the use of the dynamic membrane in wastewater, and there are still some works which focus on the micro-polluted surface water treatment [16–18]. Chu et al. [7,16] used bio-diatomite dynamic membrane reactor for micro-polluted surface water treatment, the results showed it is advantageous in high filtration flux, long filtration time, and excellent solid–liquid separation capacity, and Pollutants could be removed effectively by the reactor. But, they believed that the removal of pollutants was mainly ascribed to microbial degradation and the membrane alone; PAC-diatomite absorption was much less effective in removing pollutants.

In the present study, however, polluted river water (In China, once the river water quality fails to reach the quality set by the water environment function division, we can say the river water is polluted) was

Table 1
Summary of the five combined models at constant flow rate

Model	Equations	Parameters
Cake-complete	$P/P_0 = (1/(1 - K_b t))(1 - (K_c J_0^2/K_b)\ln(1 - K_b t))$	K_c (s/m^2), K_b (s^{-1})
Cake-complete	$P/P_0 = (1/(1 - K_b t))(1 - (K_c J_0^2/K_b)\ln(1 - K_b t))$	K_c (s/m^2), K_b (s^{-1})
Cake-intermediate	$P/P_0 = \exp(K_i J_0 t)(1 + (K_c J_0/K_i)(\exp(K_i J_0 t) - 1))$	K_c (s/m^2), K_i (m^{-1})
Complete-standard	$P/P_0 = 1/[(1 - K_b t)(1 + (K_s J_0/2K_b)\ln(1 - K_b t))^2]$	K_b (s^{-1}), K_s (m^{-1})
Intermediate-standard	$P/P_0 = \exp(K_i J_0 t)/(1 - (K_s/2K_i)(\exp(K_i J_0 t) - 1))^2$	K_i (m^{-1}), K_s (m^{-1})
Cake-standard	$P/P_0 = ((1 - K_s J_0 t/2)^{-2} + K_e J_0^2 t)$	K_c (s/m^2), K_s (m^{-1})

first coagulated in the reactor to form relatively large aggregated particles, which were subsequently separated from the water by undergoing dynamic membrane filtration. The formation of a dynamic membrane was evaluated, according to the effluent turbidity at constant flow rate. The performance of the pollutants removal was also investigated. The combined blocking models were used to identify the filtration process at constant flow rate, based on the individual model fitting parameters.

2. Materials and methods

2.1. Modeling

In this section, the five combined models of membrane fouling models are summarized, based on the Refs. [8,10,11] in Table 1 at constant flow rate.

2.2. Dynamic membrane reactor

Fig. 1 shows the experimental setup used in this study. The reactor was made of organic glass, and its effective volume was 24 L. The membrane module was constructed from polyvinyl chloride boards, bolted together with wire netting, and with a nonwoven fabric filter on two sides. The water flowed through the fabric, and out the effluent pipe. The reactor was divided into two parts by a clapboard, placed 10 cm above the bottom of the reactor. To the left of the clapboard, the coagulant was mixed with raw water by aeration through the perforated tube. In the running process, left aeration mixed the coagulant with the raw water, while right aeration idled until membrane backwashing was needed. These two aeration pipes worked in turn. The left aeration caused the water to move clockwise around the clapboard in the reactor, except during membrane backwashing. Because of the lowest water level above the horizontal effluent pipe, the effluent is passively discharged and no effluent pump is needed, unlike typical membrane bioreactors. In the running process the initial membrane flux is 100 L/(m^2 h), the intake peristaltic pump was set to this constant rate until the membrane was needed to backwash. In this constant flux, $\triangle H$ was varied from 0 to 8 cm. When $\triangle H$ reaches 8 cm, the dynamic membrane needed to backwash. After backwash is finished, a whole run cycle ended. There is a ruler outside of the reactor, the transmembrane pressure (TMP) can be easily read out through scale difference.

General characteristics of the membrane are listed in Table 2.

There is a float in the bottom pot with markers for the time that the water level indicates.

2.3. Analyses

Raw water was derived from a polluted river (QuanFu River, Jinan, China). It was fed to the reactor after simple sedimentation. Based on the characteristics of the sampling river, and early monitoring of our group, COD_{Cr}, total phosphorus (TP), and turbidity were monitored regularly by manual sampling of the influent and effluent. All the analyses were conducted according to Chinese NEPA Standard Methods [19]. Turbidity was measured with a portable turbidity-meter (HACH 2100P).

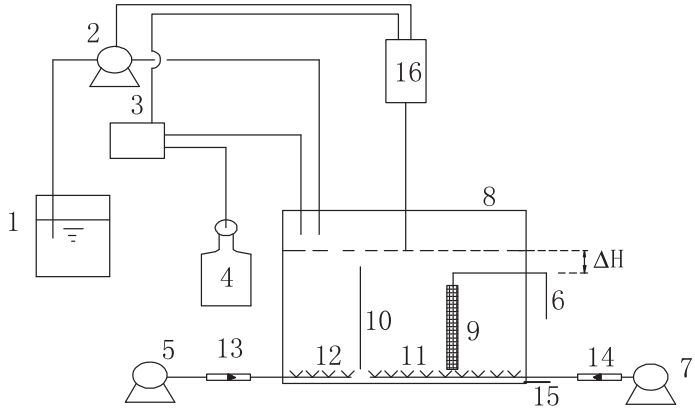

1. Storage tank for raw water 2. Intake peristaltic pump 3. Coagulant peristaltic pump 4. Storage tank for coagulant 5. Air supply pump 6. Effluent pipe 7. Air supply pump 8. Reactor 9. Membrane module 10. Baffle plate 11 and 12. Perforated aeration pipe 13 and 14. Gas flowmeter 15. Sludge withdraw pipe 16. Water level sensor

Fig. 1. Schematic diagram of the lab-scale experimental system.

Table 2
General characteristics of the membrane reactor

Configuration	Plate membrane
Material	Non-woven fabric filter (polyester fibre), dacron mesh (polyester fibre)
Cross-sectional area per membrane module	0.025 m^2
Hydrophilicity	Non-woven fabric filter (hydrophilic), dacron mesh (hydrophilic)
Number of membrane modules	3
Dacron mesh pore size	150 μm
Non-woven fabric filter weight	450 g/m^2
Dacron mesh weight	25 g/m^2
Size of each membrane module	0.11 m × 0.11 m

2.4. Jar test procedures

Coagulation experiments were carried out using jar test apparatus (DC-506 laboratory stirrer). Wastewater (1,000 ml) was dosed with commercial liquid coagulant. During coagulant addition, the solutions were first stirred rapidly at 200 rpm for 1 min, followed by slow stirring at 40 rpm for 40 min and 10 min sedimentation. The samples were taken from an outlet located 2 cm below the surface of the water. Polyaluminum chloride (PAC, Al_2O_3, 30%), polyaluminum ferric chloride (PAFC, $Al_2O_3 \geqslant 7.0\%$, $Fe^{3+} \geqslant 6.0\%$), and polyferric sulfate (PFS, $Fe^{3+} \geqslant 10\%$) were first used as the tested coagulants, during experiments. Based on the coagulation results, PAC was then selected and its optimal dose is 100 mg/L.

3. Results and discussion

3.1. System performance in pollutants removal

Turbidity in the effluent decreased dramatically over each running cycle, regardless of the initial influent turbidity (Fig. 2). A steady turbidity of the effluent indicates the build-up of a dynamic membrane. Generally, 5 NTU in effluent indicates the formation of a dynamic membrane [20]. When the turbidity in the influent was 149 NTU and 162 NTU, 5 NTU effluent was obtained after 50 min of operation. When the influent turbidity was low (60 NTU, 18 NTU and 43 NTU), merely 10 min was needed to reach an effluent turbidity of 5 NTU. Based on the results, 50 min is generally needed to form a dynamic membrane, and

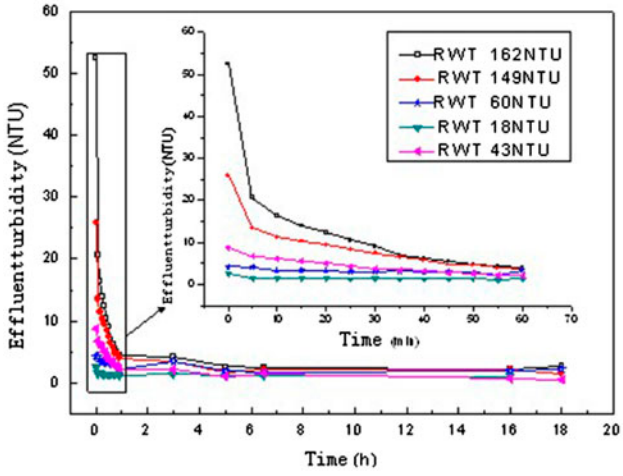

Fig. 2. Effluent turbidity over running cycles. (Inset: expanded view, 0–60 min, RWT—raw wastewater turbidity.)

if there is low turbidity in influent, less time is needed. This may be related to the marker of the dynamic membrane formation. At a different raw water quality, the same dosage of PAC, when there is lower turbidity in the influent, little time is needed to reach the 5 NTU in effluent.

When PAC is dosed into raw water, it is hydrolyzed immediately into many ionic species, including the monomers Al^{3+}, $Al(OH)^{2+}$, $Al(OH)^{2+}$, $Al(OH)_3(am)$, and $Al(OH)^{-}_4$, as well as a dimer $(Al_2(OH)_4)^{4+}$, a trimer $(Al_3(OH)_4)^{5+}$, and the tridecamer $(Al_{13}O_4(OH)_{24})^{7+}$ [21]. These cationic species adsorb negatively charged particles, decrease or neutralize the electric charge on suspended particles or zeta potential, destabilize the colloidal materials and cause the small particles to aggregate into larger settleable flocs. Because the water level in the reactor was higher than the effluent pipe, water was discharged at the hydraulic pressure. When these flocs pass through the non-woven fabric filter supported on the wire netting, most flocs stayed on the filter and the dynamic membrane was formed in a short time. Since a large pore size filter (100 μm) was used, fine flocs were discharged with the raw water at the initial stage, which can explain the high turbidity in the effluent at the initial stage. After the formation of a dynamic membrane, the membrane can accumulate fine particles, and the pollutants are removed.

Fig. 3 shows organic matter removal in terms of COD over several running cycles, when PAC was used as coagulant. The COD removal efficiency is above 65% after 10 min, independent of the different initial influent COD, and after 60 min, the COD removal of all the samples was above 70%.

According to Fig. 4, TP removal is as high as expected, based on the jar tests with no significant difference at different influent phosphorus concentrations. After the formation of a dynamic membrane, the removal efficiency of TP is above 80% with effluent concentrations less than 0.7 mg/L TP at 100 mg/L PAC, and all the effluent TP concentrations were lower than 1 mg/L TP. It is generally assumed that orthophosphate is removed by the precipitation of phosphate with the metal ion, while the total phosphorus is removed by a more complicated combination of interaction and adsorption with the flocculated particles [22,23].

Fig. 5 shows the relationship of water head, flux, and TMP of DM with the running time; it revealed that after 12 h operation, the flux of DM is almost zero, TMP of DM is almost $0.0037\,m^{-1}$, and water head reaches the set value (8 cm). This, maybe, can explain why after 16 h operation, the COD and TP removal efficiencies decreased; the reason may be related to the broken-off or drop-out part of the formed dynamic membrane, because DM is needed to be backwashed.

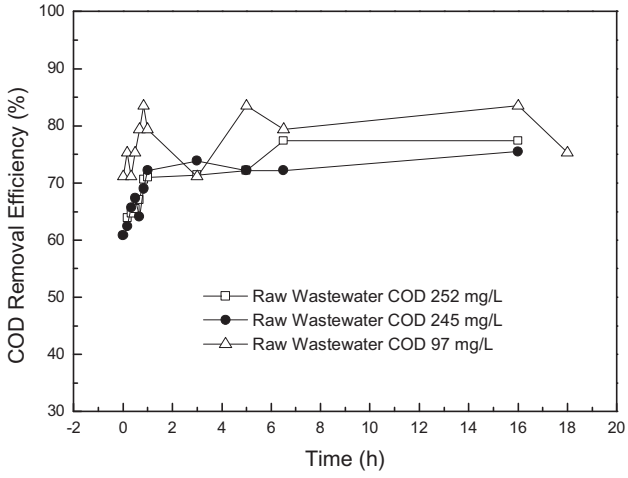

Fig. 3. COD removal over running cycles.

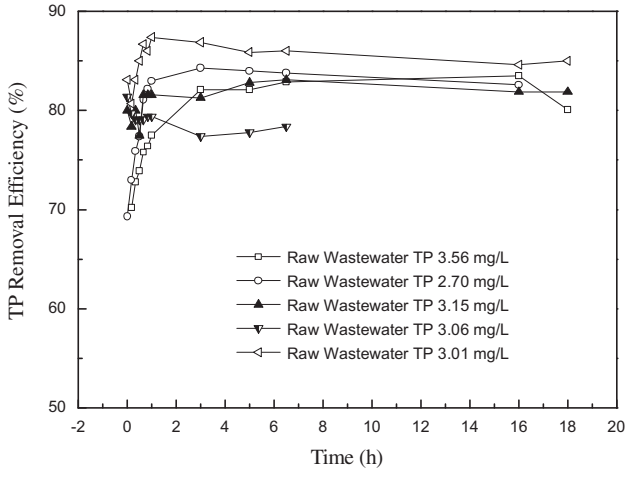

Fig. 4. Total phosphorus removal over multiple running cycles.

3.2. Coagulation–dynamic membrane filtration process

The experimental results are presented, which were conducted under the initial membrane flux $100\,L/(m^2\,h)$, when non-woven fabric filter was used as the support media of dynamic membrane. The data of pressure as a function of time, are plotted in black line in Fig. 6 and the dashed curves are the fitting curves of the typical models in the filtration of the dynamic membrane.

Fig. 6 shows that there are two distinct stages in the whole operating period. In the first period lasting for about 10 h, the pressure increasing rate is about 4.72 pa/h, then there is a shaping pressure increase. The second period was prolonged to 10 h, and the pressure increasing rate was about 113.9 pa/h. The similar pressure jump phenomenon has been observed by other studies [24,25]. The pressure jump may be related to the local flux increase, with the decrease of available filtration area over the operating time. The decrease of available filtration area is caused by blocking-pore blocking or/and inner adsorption. To identify the dynamic membrane filtration, the experimental data are fitted by the cake model, intermediate model, standard blocking model, and complete model. Fig. 6 represents the results. The fitting error and parameters were summarized in Table 3. But from the value of RSS (sum of squares of difference between data and fit values), none of these models fitted the experimental well.

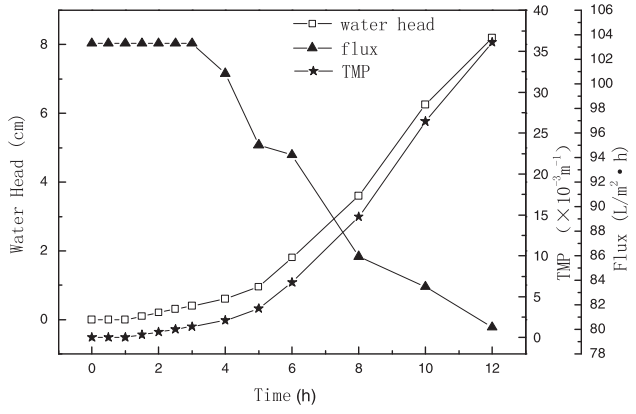

Fig. 5. The relationship of water head, flux and TMP of DM with the running time.

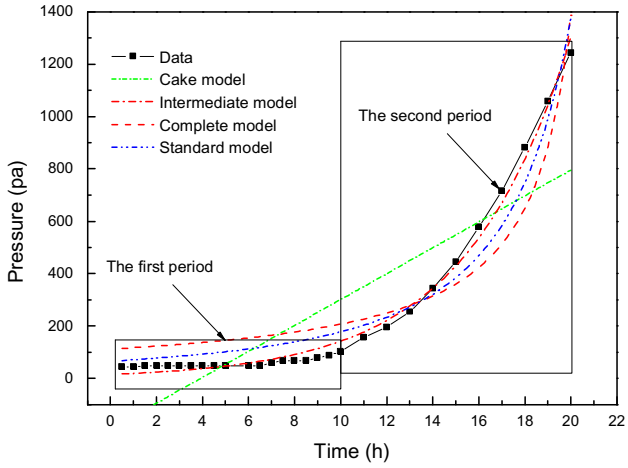

Fig. 6. Pressure as function of time when non-woven fabric filter as the support media and the cake model, the intermediate model, the standard model and the complete model fitting curves in the filtration of the dynamic membrane.

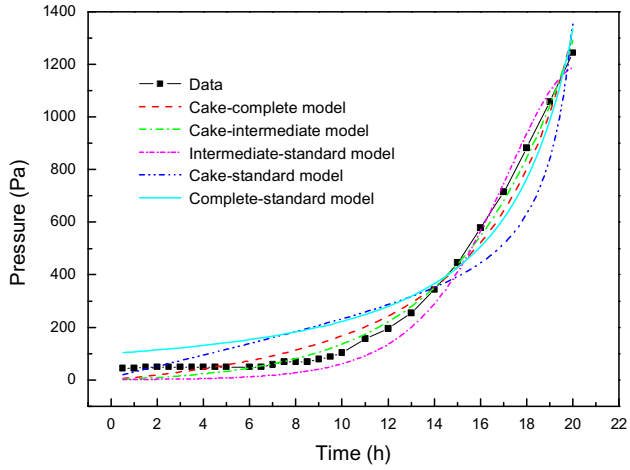

Fig. 7. Pressure as function of time using a non-woven fabric filter as the support media and the cake model. Fitting results of the combined models for the filtration of the dynamic membrane.

Table 3
Fitting error and model parameters for the cake model, the intermediate model, the complete model and the standard model in the filtration of dynamic membrane when non-woven fabric filter as the support media

Model	RSS	Fitting parameters
Cake	8.27E5	K_c 4.24E2 s/m^2
Intermediate	2.18E4	K_i 0.1062 m^{-1}
Complete	3.59E5	K_b 0.0460 s^{-1}
Standard	1.37E5	K_s 0.0622 m^{-1}

Table 4
Fitting error and model parameters for the five combined models for the filtration of the dynamic membrane using non-woven fabric filter as the support media

Model	RSS	Fitting parameters
Cake-complete	5.56E4	K_b 0.0383 s^{-1}; K_c 8.1111 s/m^2
Cake-intermediate	2.24E4	K_i 0.0971 m^{-1}; K_c 2.9955 s/m^2
Complete-standard	2.35E5	K_b 0.0377 s^{-1}; K_s 2.41E−4 m^{-1}
Intermediate-standard	5.71E4	K_i 0.4105 m^{-1}; K_s −1.71E−4 m^{-1}
Cake-standard	3.37E5	K_s 0.0898 m^{-1}; K_c 1.9954 s/m^2

And the combined models were also applied to the whole experimental period (Fig. 7). The fit error and parameters are summarized in Table 4. The fitting results showed that the combined models fit the data worse. So, these results shows that in the whole experimental period, single fouling mechanism or the single combined model is not suitable for the dynamic membrane filtration process.

Because of the existence of the two distinct stages in the whole operating period, based on the pressure changes, the fouling models are evaluated according to the relationship between running pressure and time. So, to further identify the dominant filtration mechanisms of the dynamic membrane, the typical models of membrane fouling were applied to two distinct stages: portion of the running pressure vs. time plots. Figs. 8 and 9 show the experimental data, and the fitting curves of the combined model, in the first period, and in the second period, respectively. Fitting error and model parameters are shown in Tables 5 and 6.

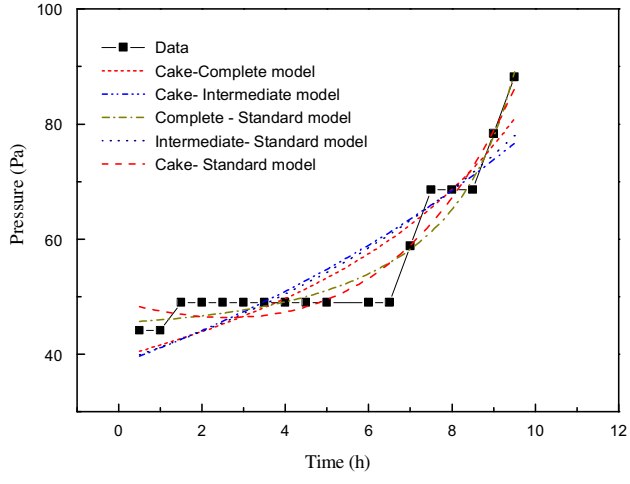

Fig. 8. In the first period the running pressure as a function of time using a non-woven fabric filter as the support media. Fitting curves of the combined models for the dynamic membrane filtration.

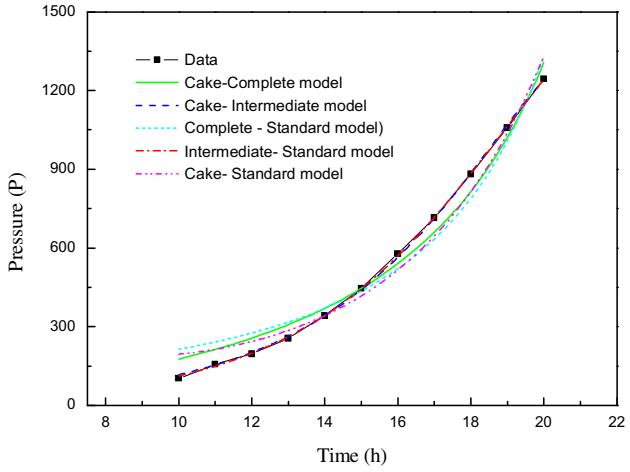

Fig. 9. In the second period the running pressure as a function of time using a non-woven fabric filter as the support media. Fitting curves of the combined models for the filtration of the dynamic membrane.

Table 5
Fitting error and model parameters for the five combined models for the filtration of the dynamic membrane using a non-woven fabric filter as the support media in the first period

Model	RSS	Fitting parameters
Cake-Complete model	412.8	K_c −50.10 s/m^2; K_b 0.0690 s^{-1}
Cake-intermediate model	595.8	K_c 4.36E-5 s/m^2; K_i 0.0079 m^{-1}
Complete-standard model	172.6	K_b 0.0902 s^{-1}; K_s 0.0198 m^{-1}
Intermediate-standard model	532.8	K_i 7.72E-7 m^{-1}; K_s 0.0959 m^{-1}
Cake-standard model	181.8	K_c −59.48 s/m^2; K_s 1.9038 m^{-1}

The fitting results of the first period (Fig. 8 and Table 5) showed that the experimental data in the first period fit better than the whole experimental period. But, the cake-standard model was as good as the fits of the complete-standard model. The contributions of intermediate blocking, standard blocking, complete blocking or caking, to the combined model were evaluated from the values of K_i, K_s, K_b/J_0 and K_cJ_0. The terms of K_i, K_s, K_b/J_0 and K_cJ_0 have units of m^{-1} and will be of similar magnitude, when their contributions to the combined model are similar [11]. For the cake-standard model, the value of K_c is negative, indicating the standard model plays the dominant role. For complete-standard model, because of the terms of K_b/J_0 and K_s have units of m^{-1} and will be of similar magnitude, the value of K_b/J_0 is 2.51E−4 m^{-1}, the ratio of $K_s/(K_b/J_0)$ is 79, which indicates the standard model was a major component in complete-standard model. Although the cake-standard model were as good as the fits of the complete-standard model, the values of K_b/J_0, K_s, K_c present in the standard model plays the dominant role in the first period. This can be explained, why in this period the pressure is slowly compared with the second period. To the standard model, the relationship of P and the initial P_0, as a function of time can be described by Eq. (1).

Table 6
Fitting error and model parameters for the five combined models for the filtration of the dynamic membrane using a non-woven fabric filter as the support media in the second period

Model	RSS	Fitting parameters
Cake-Complete model	3.01E4	K_c 2.3568 s/m^2; K_b 0.0375 s^{-1}
Cake-intermediate model	720	K_c −4.55 s/m^2; K_i 6.3712 m^{-1}
Complete-standard model	5.93E4	K_b −4.23E-7 s^{-1}; K_s 0.196 m^{-1}
Intermediate-standard model	325	K_i 0.48629 m^{-1}; K_s −8.90E-4 m^{-1}
Cake-standard model	3.72E4	K_c −54.17 s/m^2; K_s 1.21909 m^{-1}

$$\frac{P}{P_0} = \left(1 - \frac{K_s J_0 t}{2}\right)^{-2} \quad (1)$$

$$\frac{P}{P_0} = \exp(K_i J_0 t) \quad (2)$$

The fitting results of the second period (Fig 9 and Table 6) showed that the cake-intermediate model, and the intermediate-standard model fit better than the other combined models. But the fits of the cake-intermediate model was as good as that of the intermediate-standard model. The contributions of caking, intermediate blocking, or standard blocking to the combined model were evaluated from the values of K_cJ_0, K_i and K_s. The terms of K_cJ_0 and K_s have units of m^{-1} and will be of similar magnitude when their contributions to the combined model are similar [11]. For the cake-intermediate model, the value of K_c is negative, indicating the intermediate model plays the dominant role. For intermediate-standard model, because the value of K_s is negative, it indicates the

intermediate model was a major component in intermediate-standard model. In the second period, although fit of the the cake-intermediate model was as good as that of the intermediate-standard model, the values of K_cJ_0, K_i and K_s present in the intermediate model plays the dominant role. This can explain why in the second period the pressure has a high increasing rate compared with the first period. To the intermediate model, the relationship of P and the initial P_0 is pressure as a function of time can be described by Eq. (2).

4. Conclusions

The study evaluated the performance of pollutants' removal in the combined coagulation/dynamic membrane reactor. The results showed that the combined process is effective in treating polluted river water. After 50 min at higher influent turbidity, and only 10 min at lower influent turbidity, a dynamic membrane is formed. After 10-min and 60-min operations, the COD removal efficiencies were above 65% and 70%, respectively. The TP concentration in the effluent was less than 0.7 mg/L after the formation of a dynamic membrane, and all the effluent TP concentrations were below 1 mg/L. Based on the variation of the operation pressure, two distinct stages were divided. In the first stage, the pressure increasing rate is about 4.72 pa/h; the standard model plays the dominant role. For the second stage, the pressure increasing rate is about 113.9 pa/h, and the intermediate model plays the leading role.

Acknowledgments

This research was supported by the National Natural Science Foundation of China (Grant No. 51,102,157) and the Jinan Science and Technology Bureau (No. 201,102,042). This study was also funded by National Major Special Technological Programs Concerning Water Pollution Control and Management in the Twelfth Five-year Plan Period (No. 2012 ZX07203-004).

Nomenclature

J_0	—	initial flux (m/s)
K_b	—	complete blocking constant (s^{-1})
K_c	—	cake filtration constant (s/m^2)
K_i	—	intermediate blocking constant (m^{-1})
K_s	—	standard blocking constant (m^{-1})
P	—	pressure (kg/ms^2)
P_0	—	initial pressure (kg/ms^2)
t	—	time (s)

References

[1] M.H. Al-Malack, G.K. Anderson, Formation of dynamic membranes with crossflow microfiltration, J. Membr. Sci. 112 (1996) 287–296.
[2] M.H. Al-Malack, G.K. Anderson, A. Almasi, Treatment of anoxic pond effluent using crossflow microfiltration, Water Res. 32 (1998) 3738–3746.
[3] W. Fuchs, C. Resch, M. Kernstock, M. Mayer, P. Schoeberl, R. Braun, Influence of operational conditions on the performance of a mesh filter activated sludge process, Water Res. 39 (2005) 803–810.
[4] R. Jiraratananon, D. Uttapap, C. Tangamornsuksun, Self-forming dynamic membrane for ultrafiltration of pineapple juice, J. Membr. Sci. 129 (1997) 135–143.
[5] G.T. Seo, B.H. Moo, T.S. Lee, T.J. Lim, I.S. Kim, Non-woven fabric filter separation activated sludge reactor for domestic wastewater reclamation, Water Sci. Tech. 147 (2002) 133–138.
[6] Y. Kiso, Y.J. Jung, T. Ichinari, M. Park, T. Kitao, K. Nishimura, K.S. Min, Wastewater treatment performance of a filtration bio-reactor equipped with a mesh as a filter material, Water Res. 34 (2000) 4143–4150.
[7] H.Q. Chu, D.W. Cao, B.Z. Dong, Z. Qiang, Bio-diatomite dynamic membrane reactor for micro-polluted surface water treatment, Water Res. 44 (2010) 1573–1579.
[8] G. Bolton, D. LaCasse, R. Kuriyel, Combined models of membrane fouling: Development and application to microfiltration and ultrafiltration of biological fluids, J. Membr. Sci. 277 (2006) 75–84.
[9] M. Hlavacek, F. Bouchet, Constant flowrate blocking laws and an example of their application to dead-end microfiltration of protein solutions, J. Membr. Sci. 82 (1993) 285–295.
[10] J.A. Suarez, J.M. Veza, Dead-end microfiltration as advanced treatment for wastewater, Desalination 127 (2000) 47–58.
[11] Q.F. Liu, S.H. Kim, Evaluation of membrane fouling models based on bench-scale experiments: A comparison between constant flowrate blocking laws and artificial neural network (ANNs) model, J. Membr. Sci. 310 (2008) 393–401.
[12] B. Fan, X. Huang, Characteristics of a self-forming dynamic membrane coupled with a bioreactor for municipal wastewater treatment, Environ. Sci. Technol. 36 (2002) 5245–5251.
[13] M.M. Sharp, I.C. Escobar, Effects of dynamic or secondary-layer coagulation on ultrafiltration, Desalination 186 (2006) 239–249.
[14] M.H. Al-Malack, G.K. Anderson, Crossflow microfilitration with dynamic membranes, Water Res. 31 (1997) 1969–1979.
[15] J. Zhang, X.L. Han, B. Jiang, X.F. Qiu, B.Y. Gao, A hybrid system combining self-forming dynamic membrane bioreactor with coagulation process for advanced treatment of bleaching effluent from straw pulping process, Desalin. Water Treat. 18 (2010) 212–216.
[16] H.Q. Chu, B.Z. Dong, Y.L. Zhang, X.F. Zhou, Z.X. Yu, Pollutant removal mechanisms in a bio-diatomite dynamic membrane reactor for micro-polluted surface water purification, Desalination 293 (2012) 38–45.
[17] H.Q. Chu, B.Z. Dong, Y.L. Zhang, X.F. Zhou, Gravity filtration performances of the bio-diatomite dynamic membrane reactor for slightly polluted surface water purification , Water Sci. Tech. 66 (2012) 1139–1146.
[18] H.Q. Chu, Y.L. Zhang, B.Z. Dong, X.F. Zhou, D.W. Cao, Z.M. Qiang, Z.X. Yu, H.W. Wang, Pretreatment of micro-polluted surface water with a biologically enhanced PAC-diatomite dynamic membrane reactor to produce drinking water, Desalin. Water Treat. 40 (2012) 84–91.
[19] S.E.P.A. Chinese, Water and Wastewater Monitoring Methods, fourth ed., Chinese Environmental Science Publishing House, Beijing, China, 2002.
[20] X. Wu, F.T. Chen, X. Huang, Operating characteristics of self-forming dynamic membrane, Chin. Water Wastewater 20 (2004) 5–7, (in Chinese).
[21] O.S. Amudaa, I.A. Amoob, Coagulation/flocculation process and sludge conditioning in beverage industrial wastewater treatment, J. Hazard. Mater. 141 (2007) 778–783.

[22] D.J. De Renzo, Nitrogen control and Phosphorus removal in Sewage Treatment, Noyes Data Corporation. New Jersey, NJ, 1978, pp. 442–446.
[23] M.D. Elia, A. Isolati, Observed synergistic effects of aluminium and iron salts in nutrients removal, in: Proceedings of the Fifth Symposium on Chemistry of Water and Wastewater Treatment II, Gothenburg, 1992, pp. 389–400.
[24] B.O. Cho, A.G. Fane, Fouling transients in nominally sub-critical flux operation of a membrane bioreactor, J. Membr. Sci. 209 (2002) 391–404.
[25] S. Ognier, C. Wisniewski, A. Grasmick, Membrane bioreactor fouling in sub-critical filtration conditions: A local critical flux concept, J. Membr. Sci. 229 (2004) 171–177.